Bull. Disas. Prev. Res. Inst., Kyoto Univ., Vol. 21, Part 4, No. 195, March, 1972

A Wind Tunnel Model Experiment of Wind Loading on Curved Roofs

By Hatsuo Ishizaki and Yuzo Yoshikawa

(Manuscript received January 20, 1972)

Abstract

For designing structures with suspended roofs, the knowledge of the characteristics of wind forces on them is most essential, because the effect of wind forces is more serious than on ordinary roofs. However, little is known about the characteristics of wind forces on suspended roofs. Hence, an experimental study of these was carried out on two dimensional rigid roof models of three types.

Static wind pressure coefficient distributions were obtained on roofs of five different wall heights in five different wind speeds. Dynamic wind pressures were measured on the roof of three type models. Their results are discussed.

1. Introduction

Curved roofs such as hanging and membrane structures have been used increasingly in the world in the last decade. These structural systems are advantageous in construction costs to span over great distances. However, the assessment of the design wind load, as one of the most important external forces on curved roofs, is often ambiguous. More detailed research on wind loading than heretofore is required to use curved structures effectively.

There are some difficulties in the research because the effect of the Reynolds number or the scale effect of these structures may be serious in the wind tunnel test. Notwithstanding, model studies will yield valuable informations of wind loading for prototypes. From this point of view, the present authors started the study on curved roofs with a wind tunnel experimeht of wind speed and pressure distributions on the two dimensional models. The problem of dynamic behaviors of these structures under wind actions will be also important, but we must leave this for a future study. The experiment shown in the following is only a preliminary study on curved structures of simple shape.

2. Description of the experiments

The Göttingen type wind tunnel of the Disaster Prevention Research Institute of Kyoto University was used in this experiment. The wind tunnel has an octagonal working section of 1 m in diagonal length and its wind speed can be controlled from 3 to 60 m/s.

In order to simplify the problem the experiment was made on two dimensional models with end plates. The model was placed on the ground plate in the working section which extends long enough so that it has no effect, as discussed by Leutheusser et al[1]. Turbulence generator was not used in this experiment. The schematic

diagram and dimensions of the experimental installation are shown in Fig. 1. Three types of models with the same span length of 50 cm were used: one was the flat roof type (Model-A) and other two were concavely curved roofs with maximum sag depths of 5 cm (Model-B) and 10 cm (Model-C). The parabolic curve of the roof was chosen because this is very similar to catenary curve and is typical in practical applications. As the windward wall height has great influence on the wind pressure distribution on the roof, the models with five different wall heights of 10, 12.5, 15, 17.5 and 20 cm were made for each type of the model.

Wind speed distributions over the roofs and wind pressures on them with 15 different models were measured for five different wind speeds of 5, 10, 15, 20 and 25 m/s. The positions of the measured points are along the central line of the model as shown in Fig. 2. The measuring point 1 is at 2 cm from the edge.

The sensor of the wind speed measurement was a hot-wire anemometer with 'I' probe and the pressure sensor was the strain gauge type one which can measure the dynamic pressure up to 100 cps. The reference pressure for the pressure gauge was the static pressure of the Pitot-static tube for the measurement of reference wind tunnel wind speed, as shown in Fig. 1. The outputs from the pressure gauge and the hot-wire anemometer were recorded on the multichannel pen-oscilograph, which can

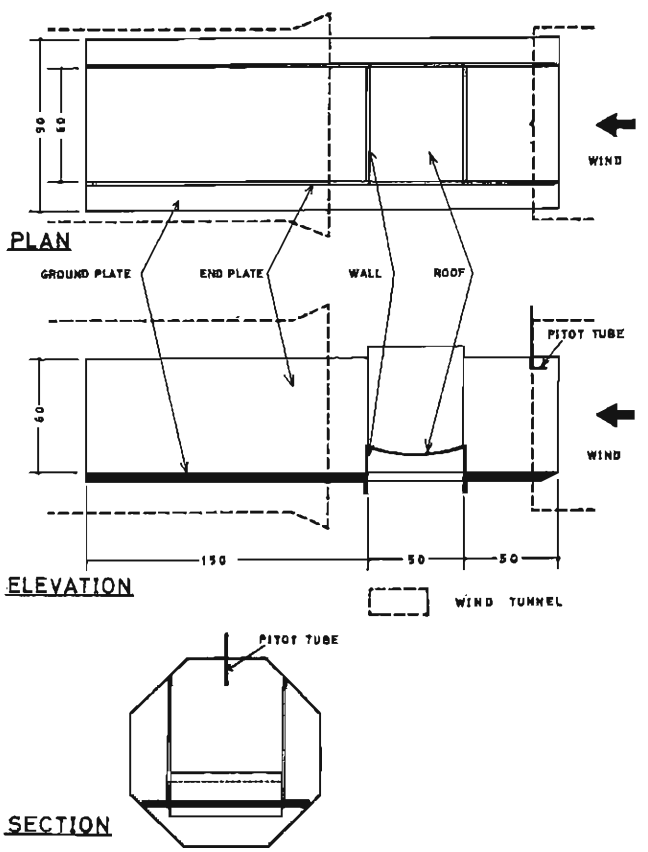

Fig. 1. Schematic of installation (unit cm).

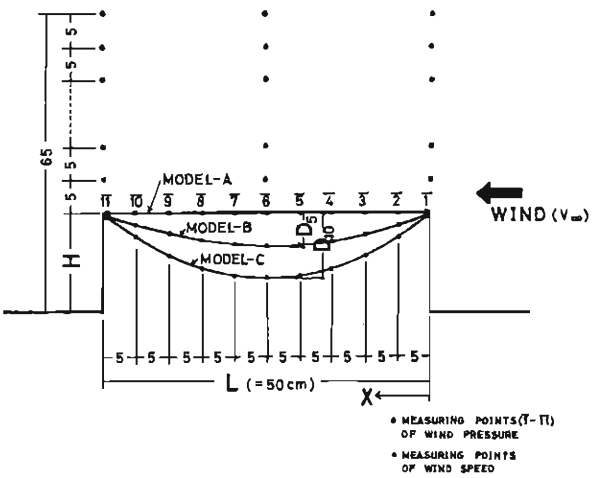

Fig. 2. Schematic of roof models and measuring positions (unit cm).

follow the inputs up to 70 cps. The traces were read manually and the data were processed by the computer KDC–2 of Kyoto University.

3. Results of experiments

3.1. Wind speed distributions

The results of the wind speed profile measurements above the points *P*, *Q*, *R* and *S* at three different wind speeds (5, 10 and 15 m/s) are shown in Figs. 3, 4 and 5. The results for two wall heights models (15 and 20 cm) for each type are shown in these figures. As a hot-wire anemometer with 'I' probe was used in the measurement, the wind speed shown in the figures are total wind speeds.

The wind speed above the windward point *P* is not affected by the model at the height higher than 40 cm. The position of the Pitot-static tube is at 55 cm high on the point *P*, which is the representative point of the free stream.

The relative wind speed distributions along the height above each point were not changed with wind speeds. However, they are affected by the wall height and the depth of the wake increases with increasing wall height. The growth of the turbulent region or wake is more rapid on the concave roof than on the flat roof.

3.2. Static wind pressure distributions

The static wind pressure coefficient distributions on the flat roof or Model-A are shown in Fig. 6. The maximum absolute values are about -1.5 and are located near the edge on the models whose wall heights are 17.5, 15, 12.5 and 10 cm, and the coefficients decrease with downward distance from the edge and tends to the value of about -0.3. In the case of the 20 cm wall height model the wind pressure coefficient at the edge is smaller than those of the lower models and show peaks at a little downward place from the edge and they decrease slowly with distance.

Figs. 7 and 8 show the distributions of the static wind pressure coefficients on the curved roofs. In these cases the distribution is more uniform over the whole roof

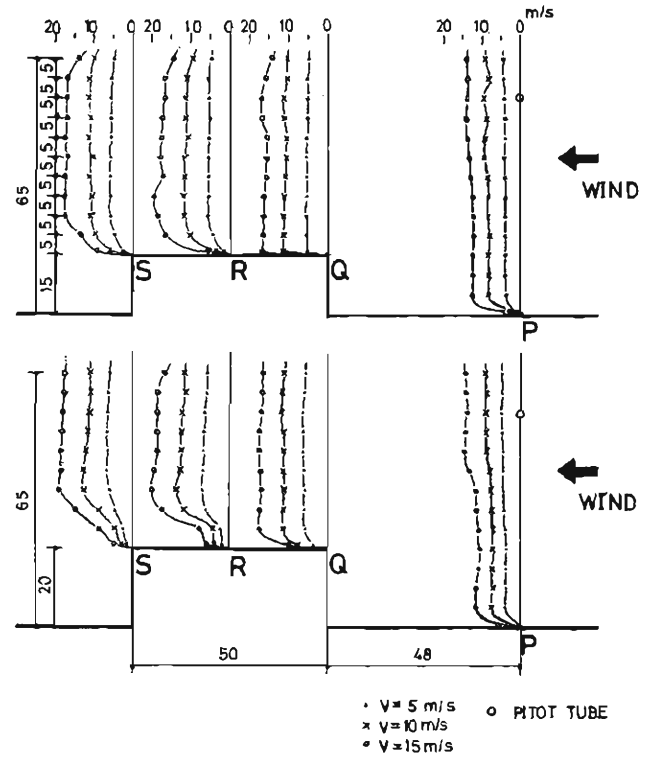

Fig. 3. Wind speed profile, Model-A (unit cm).

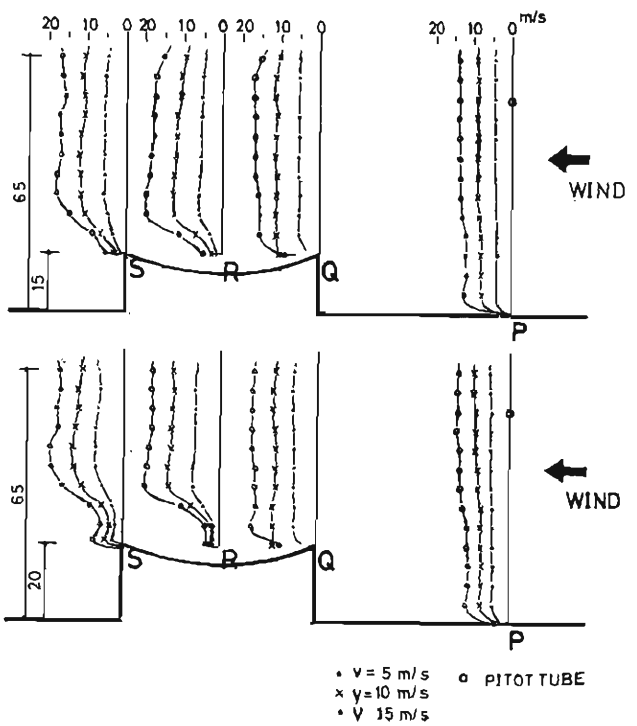

Fig. 4. Wind speed profile, Model-B (unit cm).

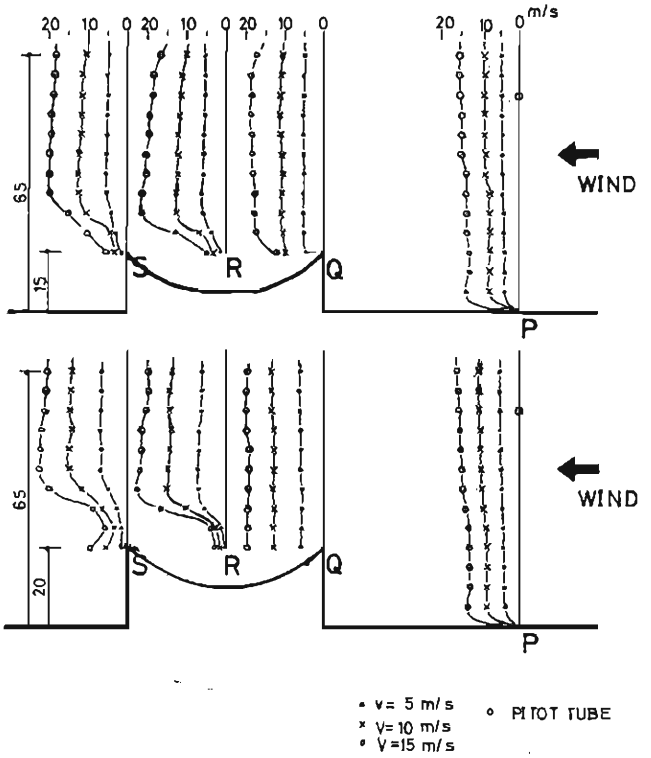

Fig. 5. Wind speed profile, Model-C (unit cm).

than in the case of the flat roof and the maximum absolute value is seen near the leeward edge on 20 cm wall height model. The maximum suction coefficients are −1.48 for Model-B type and −1.53 for Model-C type, which are smaller than −1.83 for Model-A type. The mean coefficients over the whole roof are rather larger for the curved roofs than for the flat roofs. In the cases when the wall heights are smaller, the values of the wind pressure coefficients are remarkably varied by the sag ratio. In case of the deep sag (Model-C) the peak of the absolute pressure coefficient is near the middle point or at a little on the lee side of that point, while the peak is seen between the windward edge and the middle point in the case of the shallow sag (Model-B). When the walls are higher than 15 cm, the coefficients are almost the same for the curved roofs of both types. These tendencies can be clearly seen in the summarized form of Figs. 9, 10 and 11. As distinctly seen in these figures, difference between the pressure coefficients of the flat roof and the curved roof decreases with the increasing H/L value and/or increasing wind speed.

3.3. Fluctuating wind pressure

The characteristics of the fluctuating pressures on the roof also were analyzed. The results of spectral analysis of wind pressure fluctuations on each model with 15 cm height wall in the 10 m/s wind are shown in Figs. 12, 13 and 14. The figures show the product of frequency and normalized power spectral density in logarithmic scale

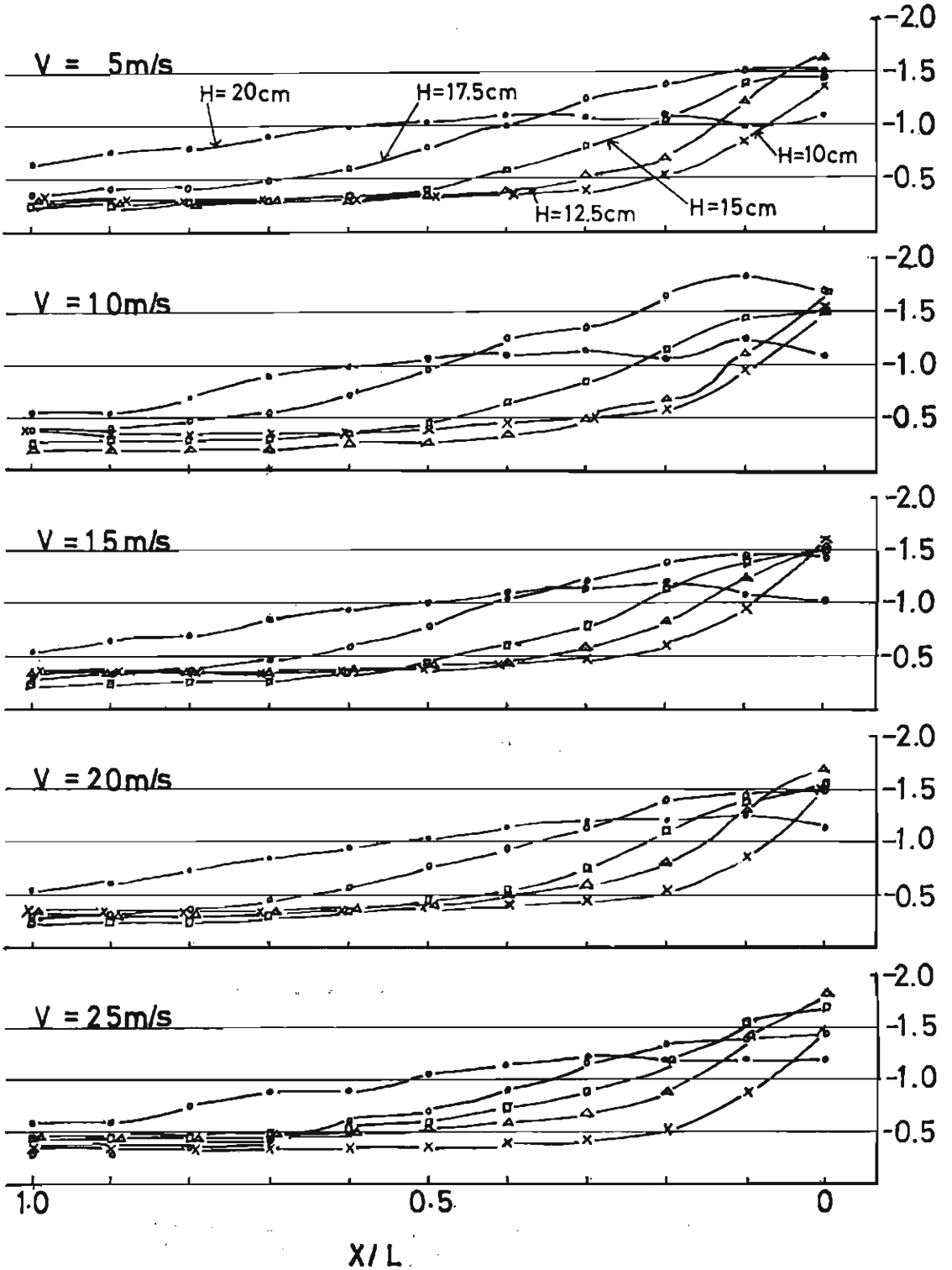

Fig. 6. Wind pressure coefficient distribution of Model-A

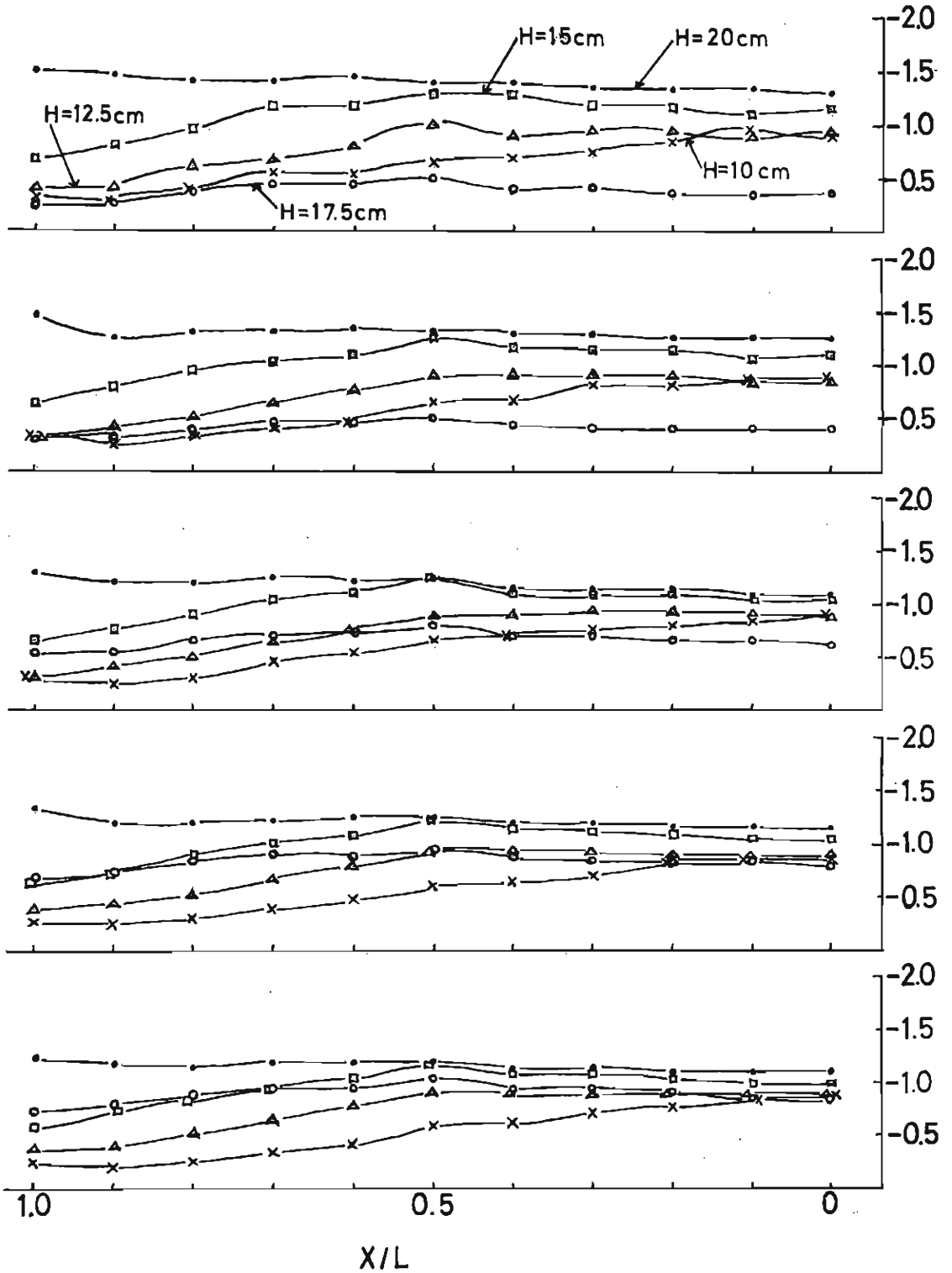

Fig. 7. Wind pressure coefficient distribution of Model-B.

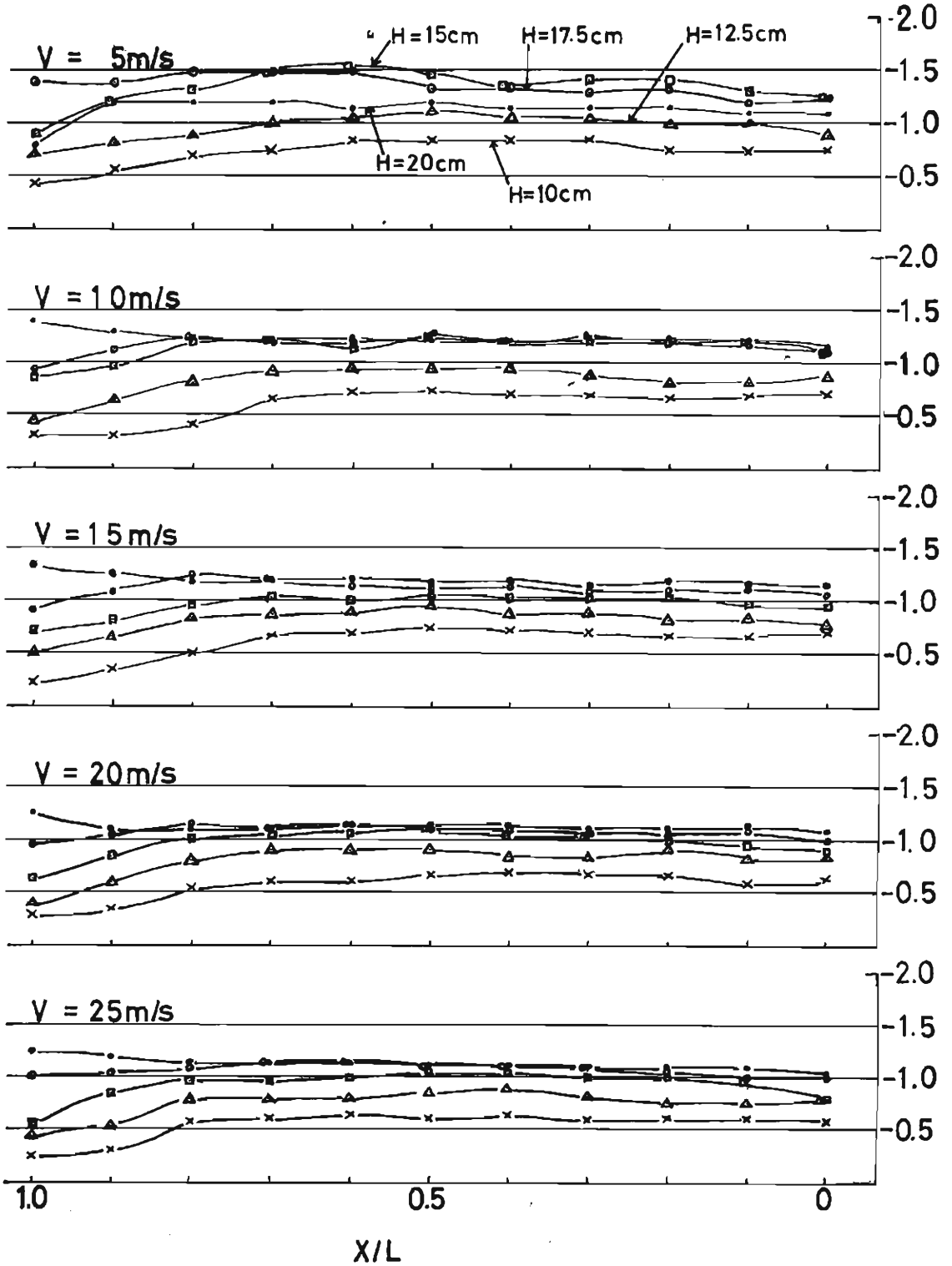

Fig. 8. Wind pressure coefficient distribution of Model-C.

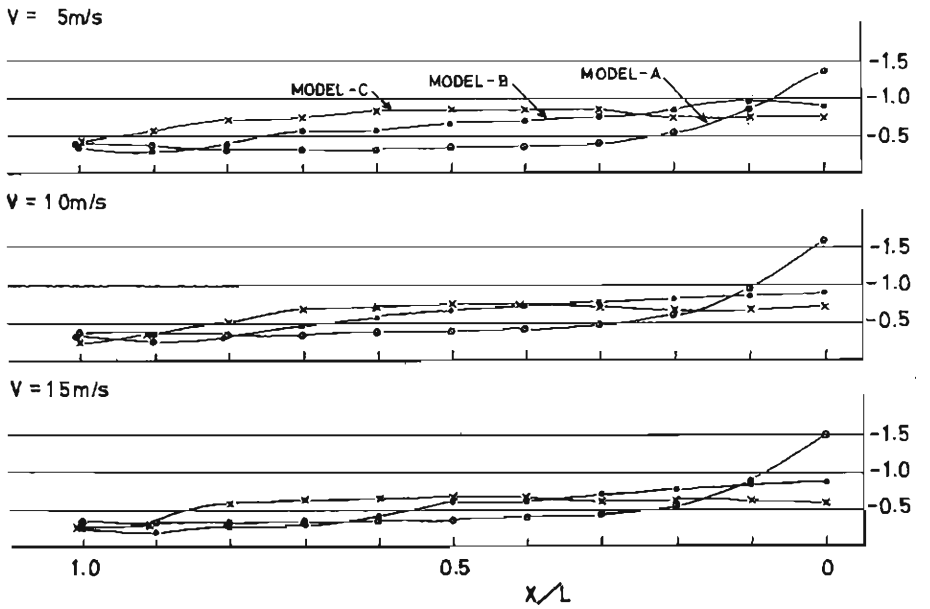

Fig. 9. Variation of the pressure distribution among the 3 models with a 10 cm wall.

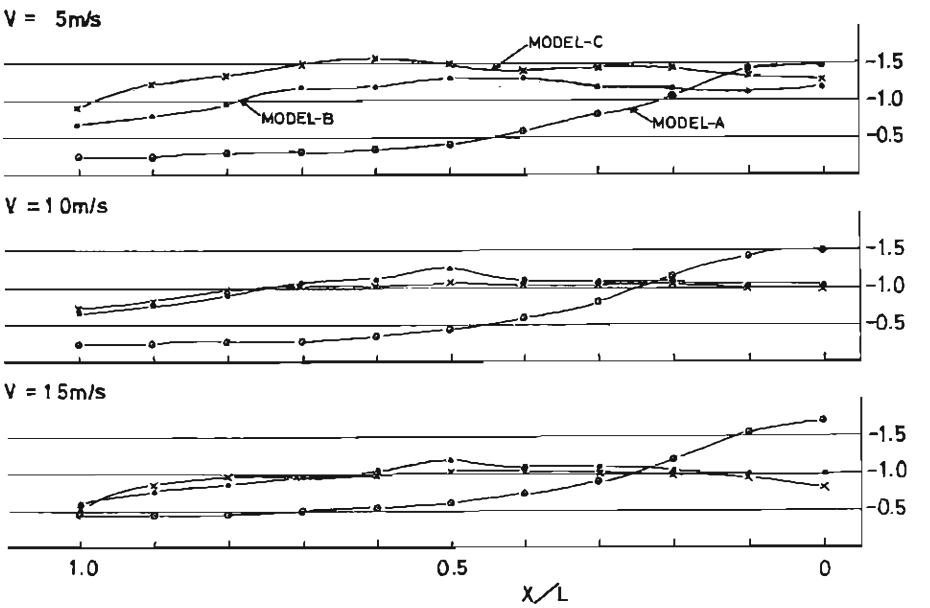

Fig. 10. Variation of the pressure distribution among the 3 models with a 15cm wall.

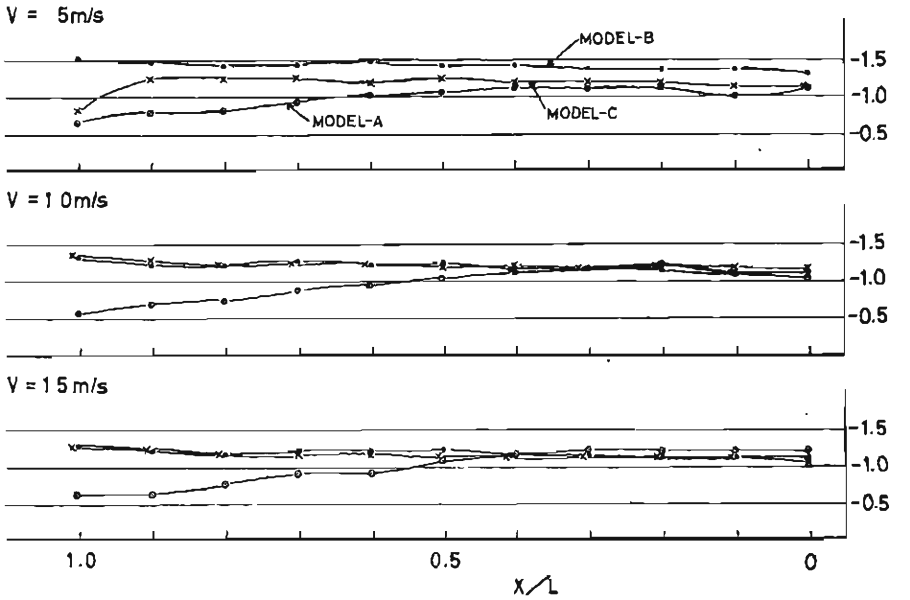

Fig. 11. Variation of the pressure distribution among the 3 models with a 20cm wall.

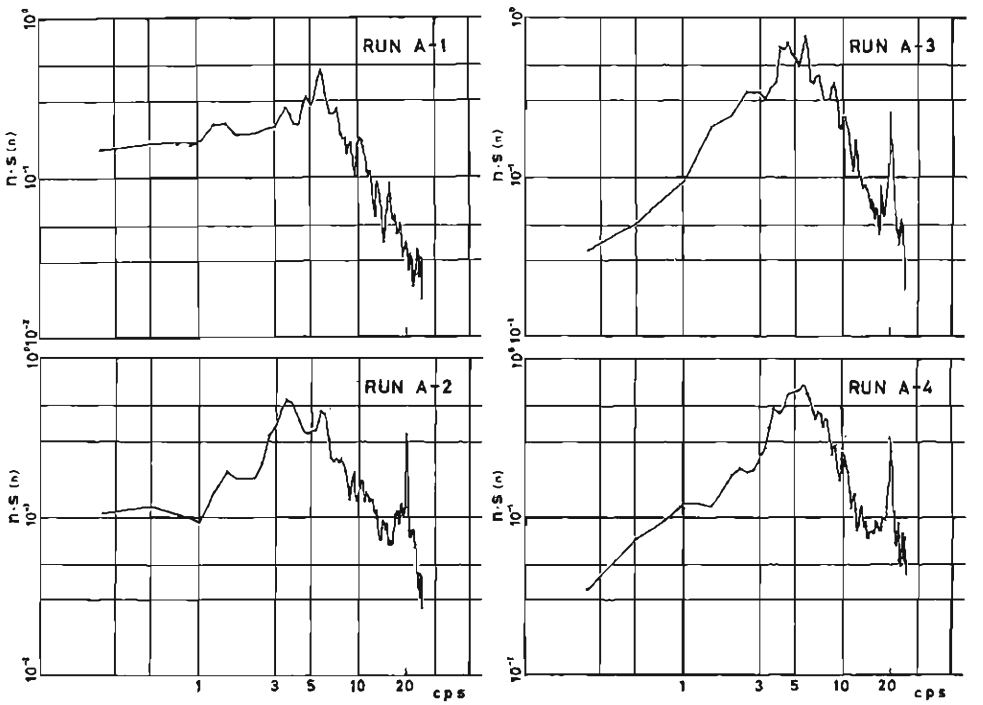

Fig. 12. Power spectrum of wind pressure (Model-A).

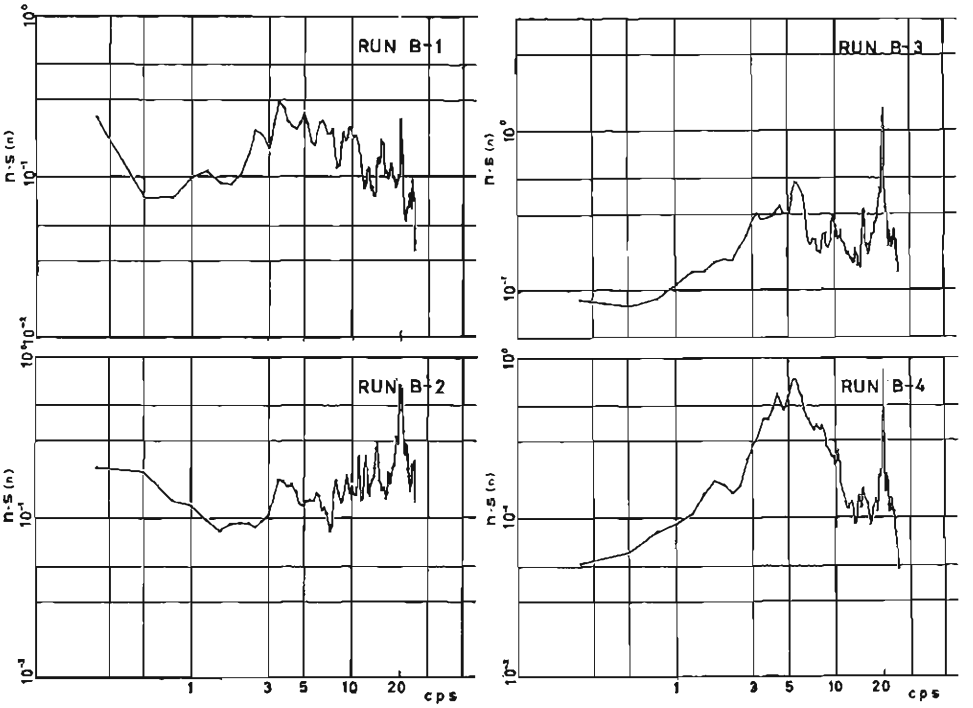

Fig. 13. Power spectrum of wind pressure (Model-B).

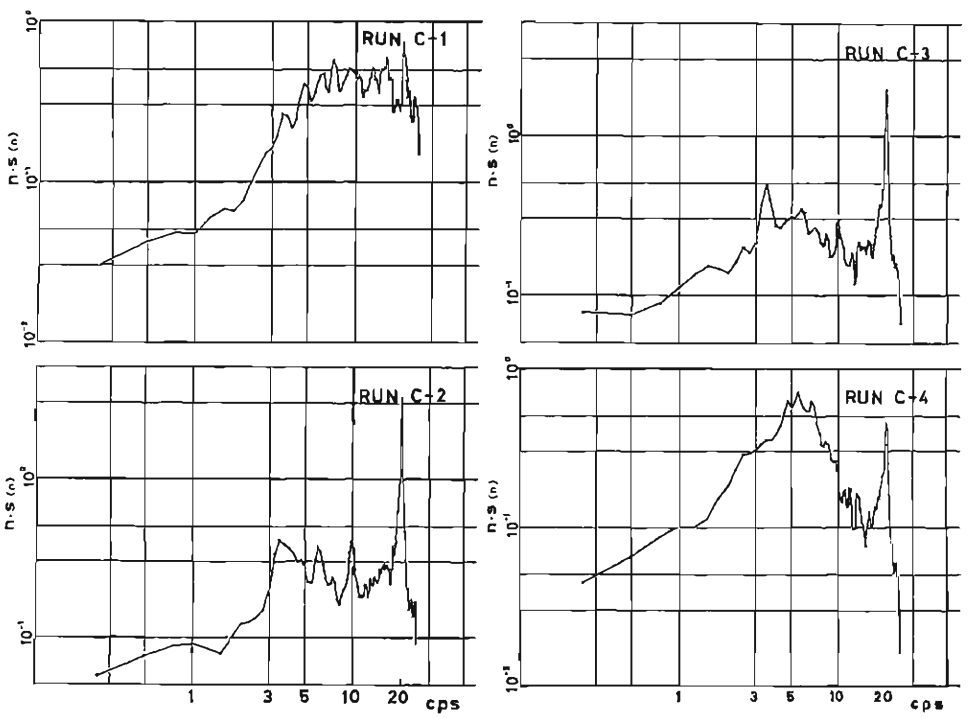

Fig. 14. Power spectrum of wind pressure (Model-C)

Table 1.

Run No.	Model	Measur. Point	Wind Pressure			Inten. Turbul.	Gust Factor
			Mean	Stand. Dev.	Max.		
			$\bar{P}$	σ_p	P_{max}	$\sigma_p/\bar{P}$	$P_{max}/\bar{P}$
			mmAq	mmAq	mmAq		
A–1	A	1	−6.07	0.39	−8.51	0.06	1.40
A–2	A	3	−4.07	0.59	−6.83	0.14	1.68
A–3	A	6	−3.40	0.58	−5.60	0.17	1.65
A–4	A	10	−1.09	0.65	−7.18	0.60	6.59
B–1	B	1	−2.31	0.36	−3.15	0.16	1.36
B–2	B	3	−3.37	0.27	−4.76	0.08	1.41
B–3	B	6	−3.24	0.33	−4.76	0.10	1.47
B–4	B	10	−3.24	0.40	−4.92	0.12	1.52
C–1	C	1	−4.21	0.22	−4.69	0.05	1.11
C–2	C	3	−3.64	0.27	−4.45	0.07	1.22
C–3	C	6	−3.65	0.30	−4.77	0.08	1.31
C–4	C	10	−4.05	0.47	−5.88	0.12	1.45

against frequency in the same scale. The related statistical parameters are shown in Table 1. The averaged intensity of the wind pressure fluctuation (standard deviation/mean value) is largest on Model-A and smallest on Model-C, and it shows that the intensity takes the maximum value on the windward edge and decreases with leeward distance on each model.

As is clear from the figures, most of the spectra of wind pressure fluctuations show a broad peak with the peak frequency around 5.8 cps and a narrow peak at 20 cps. These peak frequencies are independent of the shape of the model. The reason for the existence of frequency peak at 20 cps in all cases is not clear, but its frequency coincides with the inverse of the travelling time of the wind over the model (0.5 m/ 10 m/s). The former broad peak may correspond to the shedding of the eddy produced by the model. The nondimensional value $f(2H)/V$, where f is the peak frequency and V being the wind speed, is about 0.17. This value is comparable with the Strouhal number 0.12 with a rectangular cylinder obtained by Vickery[2], although the rectangular cylinder was mounted on the ground plate in our experiment. This broad peak is less distinct with the curved roofs especially on Model-C. And in the cases of the curved roofs minor peaks of various frequencies are seen at the points near the windward edge, but they are not seen in the spectra on the leeward points, which are not so different from type to type.

4. Discussion and concluding remarks

The difference of the roof shape causes the different wind flow pattern over the roofs as is seen in Figs. 3, 4 and 5. The dependency of the wake figure above the model is not so apparent, but the development of the wake region on the roof becomes steeper with increasing of wall height and sag depth. This may be related to the change of the wind pressure distribution on the wind speed and sag depth.

In the present experiment the largest pressure coefficient of −1.5 is measured on

the edge of the roof and the magnitude of the coefficient decreases with downward distance from the edge and tends to the value of about −0.3. The values reported by Jensen et al[3], are similar to the present result in their distribution. One example of these coefficient distributions of Model-A is shown in Fig. 15. These coefficients

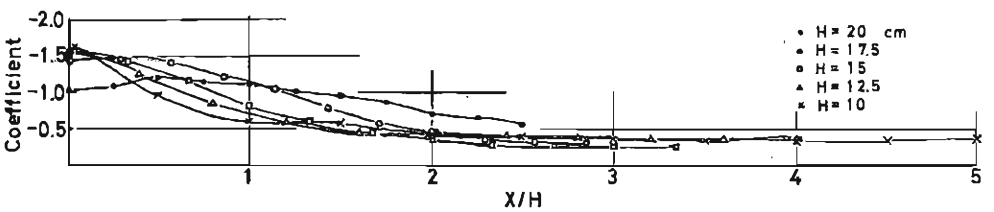

Fig. 15. Pressure coefficient distribution of Model-A (V=15m/s).

are plotted against the non-dimensional distance X/H, where X is the distance from the edge. The coefficients of the wall heights 17.5, 15, 12.5 and 10 cm are −1.5 near the edge and decreases with downward distance. And these values are the same at X/H=2. It is easily seen that the application of the value of −0.5 on the whole flat roof which is suggested by the design criteria of A.I.J.* may be an underestimation in the surface near the windward edge. In the design of the flat roof, the result of the present experiment which shows that the larger static suction will be applied on the roof surface within the range of about 2H from windward edge, must be considered. In the case of 20 cm wall height, the coefficient is −1.0 which is less than those of other height cases and −0.7 at X/H=2. The reason for this difference may be caused by the model length in the wind direction (L=50 cm).

The static wind pressure distributions on the curved roofs show the distinct difference from that of the flat roof. In the cases of the curved roofs the pressure coefficients are more uniformly distributed than in the case of the flat roof. The averaged pressure coefficient was much larger than in the case of the flat roof and which is about −0.9 on average.

Empirically, the static pressure coefficient is said to be independent of the Reynodls number. Figs. 16, 17 and 18 show the effect of wind speed on the pressure coefficient. In these figures one pressure coefficient at V=10 m/s is plotted against other pressure coefficients at V=5, 15, 20 and 25 m/s of the same wall height and the same measuring point. In the cases of Model-A and Model-B, the marks scatter near the slope of 1.0, and this shows that the effect of wind speed is small. However, this tendency becomes small on Model-C, or the pressure coefficients of the deep sag roof are affected by the wind speed.

Figs. 19, 20 and 21 show the effect of wall height on the pressure coefficient at V= 15 m/s, and the variation of coefficients with wall height is shown at six measuring points (1, 3, 5, 7, 9 and 11). In many cases the coefficient increases with wall height. These figures show the distribution too. The values of coefficients of some measuring points tend to meet together with wall height, or the distribution becomes uniform over the whole roof with wall height. This tendency is dependent on the sag depth.

* The Architectural Institute of Japan

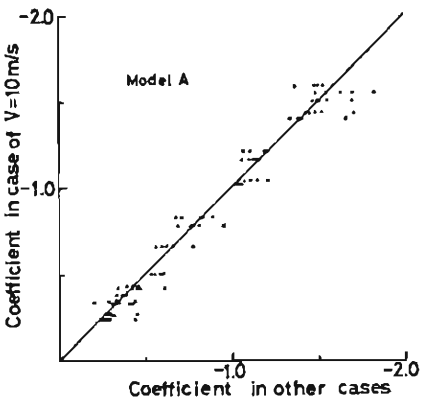

Fig. 16. Variation of pressure coefficient with wind speed (Model-A).

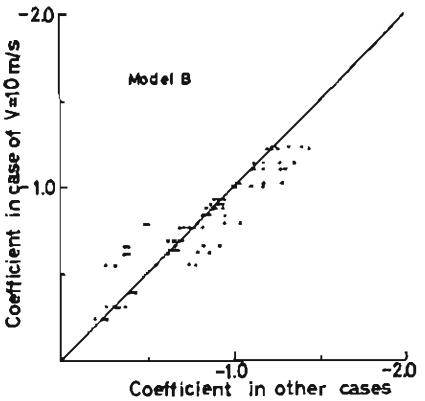

Fig. 17. Variation of pressure coefficient with wind speed (Model-B).

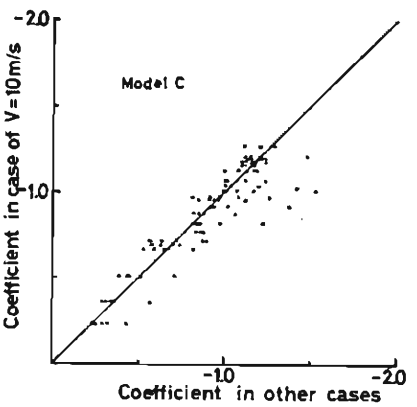

Fig. 18. Variation of pressure coefficient with wind speed (Model-C).

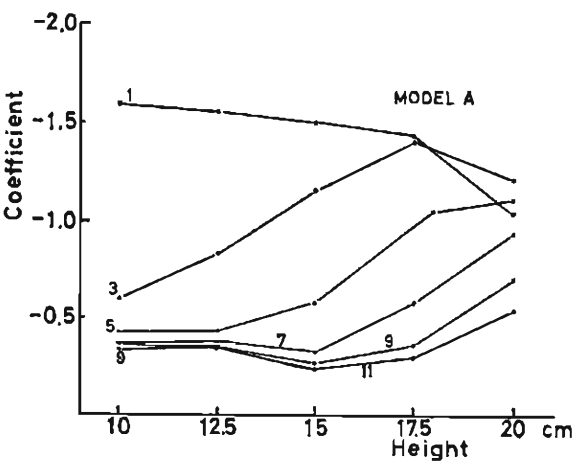

Fig. 19. Variation of coefficient of Model-A with wall height when $V=15$m/s.

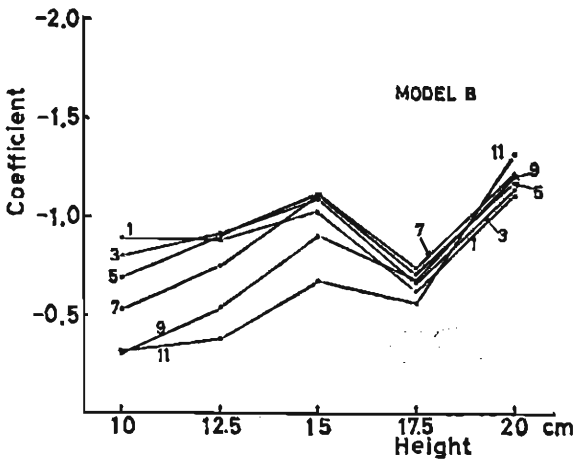

Fig. 20. Variation of coefficient of Model-B with wall height when $V=15$m/s.

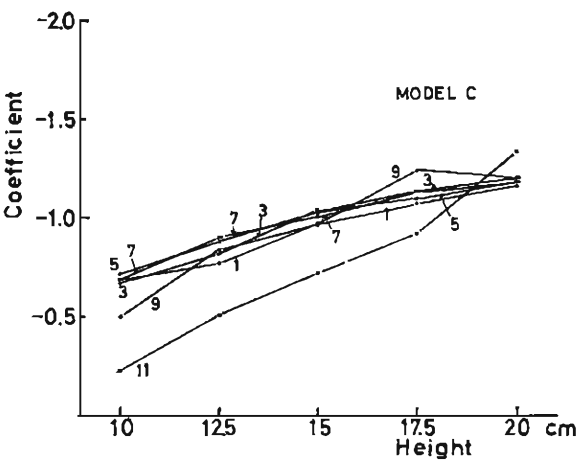

Fig. 21. Variation of coefficient of Model-C with wall height when $V=15$m/s.

As the weight of the suspended roof is usually smaller than the ordinary roof, the fluctuating component of wind pressure must be taken into account in the design. The spectral analysis of the wind pressure fluctuations on the roof shows a broad peak at 5.8 cps and a narrow sharp peak at 20 cps in all cases. The former broad peak frequency resembles the value expected from the Strouhal number of the eddy shedding from the cylinder. The non-dimensional value $f(2H)/V$ is about 0.17. This value is between the Strouhal number 0.20 for cylinder and the eddy frequency 0.12 shedding from the rectangular cylinder by Vickery. This shows that the frequency of the eddy produced by the rectangular cylinder on the ground may also be estimated by the similar relation. This peak is less distinct on the curved roofs and minor peaks of various frequencies are seen near the windward edge, but they are damped out quickly and are not found away from the edge. The cause of the latter narrow sharp peak is not explained at present. A predominent periodical pressure

fluctuation can not be seen over the whole surface of the curved roofs in the present experiment. This is favourable for the design of the roof. However, it is unfavourable for the choice of the local members that minor peaks of various frequencies were seen near the windward edge, because the region in which the local resonance may occur is wide. From the other point of view, the local fluctuation may bring the danger to the whole structure, because the local vibration is propagating as the wave.

Taking such problems into consideration, more experiment must be made on various models with various shapes and dimensions. In order to make the vibrating characteristics of the suspended roofs clear, the experiment on the vibrating model will be required.

For designing the structure with a suspended roof, the knowledge of both static and dynamic wind pressure on the roof is most essential, because the effect of wind pressure is more serious than on ordinary roofs owing to their light weight. The characteristics of wind pressure on the curved roof are scarcely known at present. For the purpose of establishing the wind load we must know the static wind pressure distribution and the dynamic component.

The fluctuating pressure on the roof $P(x, t)$ depends on the nature of the approaching flow and the dimensions of the model; the span length L, wall height H and sag depth D. The characteristics of the approaching uniform flow is governed by the free stream speed V, fluid density ρ and viscosity μ.

Thus, the dynamic pressure is a function of these parameters.

$$P(x, t)=F(x, t, V, \rho, \mu, H, L, D)$$

Choosing ρ, V and H as fundamental units,

$$\frac{P(x, t)}{\frac{1}{2}\rho V^2}=f\left(\frac{x}{H}, \frac{tV}{H}, \frac{HV}{\mu/\rho}, \frac{L}{H}, \frac{D}{H}\right)$$

For the static pressure $P(x)$, dropping the time variable.

$$\frac{P(x)}{\frac{1}{2}\rho V^2}=f\left(\frac{x}{H}, \frac{HV}{\mu/\rho}, \frac{L}{H}, \frac{D}{H}\right)$$

We changed three parameters H, D and V in this experiment. The present experiment is a preliminary work for more detailed research in future, and the results of this experiment cannot be adopted for practical design purposes. However, some suggestions were gained for our future experimental research. The distribution of pressure coefficients on the roof is dependent on the wall height in both shape and magnitude, and it is a little affected by the wind speed for the deep sag model, too. More detailed experiments are necessary on various models with more various wind speeds in order to make the relation among the wind speed, wall height, sag depth and pressure distribution clear. The measurements of dynamic pressures also must be made on various models in various wind speeds. If the non-dimensional number $f(2H)/V$ can be decided in considerations similar to the Strouhal number, this would

be beneficial in design. The measurement of wind speed fluctuation is efficient for the acquisition of the knowledge of vortex shedding from the edge. We shall advance this research starting from the present experiment.

Acknowledgement

The authors are indebted to Mr. K. Sugimasa, technical officer of Kyoto University, for his assistance in carrying out the measurement and the data analysis.

References

1) Leutheusser, H. J. and W. D. Baines: Similitude Problems in Building Aerodynamics, J. of the Hydraulics Division, Proceedings of the A.S.C.E., 1967, pp. 5226–5240.
2) Vickery, B. J.: Fluctuating Lift and Drag on a Long Cylinder of Square Cross-section in a Smooth and in a Turbulent Stream, J. Fluid Mech. 1966 Vol. 25, Part 3, pp. 481–494.
3) Jensen, M. and N. Franck: Model-scale Tests in Turbulent Wind, The Danish Technical Press, Copenhagen, 1963.